

Accepted Manuscript

Hybrid Remap for Multi-Material ALE

M. Kucharik, J. Breil, S. Galera, P.-H. Maire, M. Berndt, M. Shashkov

PII: S0045-7930(10)00197-0

DOI: [10.1016/j.compfluid.2010.08.004](https://doi.org/10.1016/j.compfluid.2010.08.004)

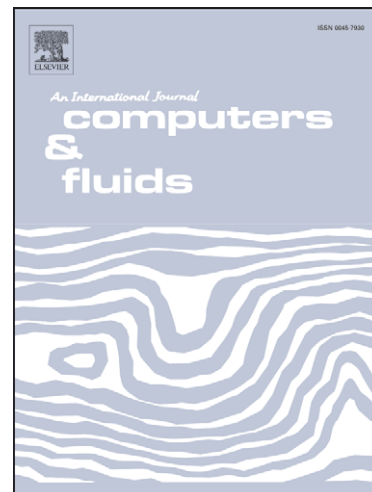
Reference: CAF 1351

To appear in: *Computers & Fluids*

Received Date: 27 April 2010

Revised Date: 15 July 2010

Accepted Date: 5 August 2010



Please cite this article as: Kucharik, M., Breil, J., Galera, S., Maire, P.-H., Berndt, M., Shashkov, M., Hybrid Remap for Multi-Material ALE, *Computers & Fluids* (2010), doi: [10.1016/j.compfluid.2010.08.004](https://doi.org/10.1016/j.compfluid.2010.08.004)

This is a PDF file of an unedited manuscript that has been accepted for publication. As a service to our customers we are providing this early version of the manuscript. The manuscript will undergo copyediting, typesetting, and review of the resulting proof before it is published in its final form. Please note that during the production process errors may be discovered which could affect the content, and all legal disclaimers that apply to the journal pertain.

Hybrid Remap for Multi-Material ALE[☆]

M. Kucharik^{*,a}, J. Breil^b, S. Galera^b, P.-H. Maire^b, M. Berndt^c,
M. Shashkov^d

^a Faculty of Nuclear Sciences and Physical Engineering, Czech Technical University in Prague, Brehova 7, Praha 1, 115 19, Czech Republic

^b UMR CELIA CEA-CNRS-Université Bordeaux I, 33 405 Talence Cedex, France

^c CCS-2 Group, MS D413, Los Alamos National Laboratory, P.O. Box 1663, Los Alamos, NM 87545, U.S.A.

^d XCP-4 Group, MS B284, Los Alamos National Laboratory, P.O. Box 1663, Los Alamos, NM 87545, U.S.A.

Abstract

Remapping is one of the essential parts of most arbitrary Lagrangian-Eulerian (ALE) methods. In this short paper we focus on multi-material fluid flows. We present a hybrid remapping method combining the swept remapping algorithm in pure regions with the intersection-based remapping algorithm close to material interfaces. We describe the hybrid remapping method in two formulations, as a one-step and a two-step procedure, and compare behavior of both approaches with the standard intersection-based algorithm using several numerical examples.

Key words: multi-material ALE, conservative interpolations, hybrid remap

1. Introduction

There exist two basic approaches for hydrodynamic simulations – Eulerian and Lagrangian methods. Eulerian methods utilize a static computational

[☆]LA-UR 10-01861

*E-mail: kucharik@newton.fjfi.cvut.cz

mesh and the fluid flows in the form of mass flux through it. In the Lagrangian framework, the computational mesh moves with the fluid and naturally follows the changing computational domain. Therefore, it is more suitable for certain types of applications including severe compressions and expansions. Due to the mesh motion, its tangling or degeneration can occur causing the failure of the simulation. In the pioneering paper [4], the Arbitrary Lagrangian-Eulerian (ALE) method was introduced, combining best properties of both approaches. The computational mesh follows the physical domain due to the embodied Lagrangian solver, while the Eulerian part (consisting of mesh rezoning followed by remapping, interpolating conservatively all fluid quantities from the Lagrangian to the rezoned mesh) keeps it smooth. The ALE approach became very popular, and many authors contributed to this topic [1, 10, 5, 12]. For real life applications, multi-material ALE must be used, allowing more materials to share the same computational cell.

We focus on the remapping stage of the multi-material ALE algorithm. There exist generally two approaches based on 1) approximate (swept) fluxes and 2) intersections. In simulations with only one material, the simple (and fast) swept approximation can be used, integrating their piecewise-linearly reconstructed densities in the swept region, defined by the motion of the particular mesh edge in the rezoning stage, see for example [9, 11, 8]. In the case when several materials are present, the rezoned mesh will include mixed cells, and the classical (intersection-based) approach must be used, in which pure material polygons of the Lagrangian mesh are intersected with the new mesh cells, and summed up to the total value of each fluid quantity

in the new cells. As intersections are used, this approach can become rather expensive in 2D and almost impossible to use in 3D. The intersection-based remapper can be also formulated in a flux form [11].

In this paper, we describe a new method that we call hybrid remapping, combining both approaches. It incorporates the cheap swept approach in pure regions and employs intersections only in the regions where more materials are present. Hence, intersections are avoided in pure regions that often cover most of the domain. This hybrid remapping approach can dramatically decrease the cost of the multi-material remap.

The rest of the paper is organized as follows. In Section 2, the 2-step hybrid remapper is discussed. It is based on a clever trick – in the first step, only pure regions are rezoned and remapped by the swept approach, while in the second step, mixed regions are treated by the intersection-based approach. In Section 3, the 1-step hybrid remapping approach is discussed, in which the mass (and other) fluxes are constructed at once, by the combination of the swept and intersection-based fluxes. In Section 4, the numerical errors and time costs of both approaches are compared with the standard methods.

2. Two-Step Hybrid Remap

In the two-step hybrid remapping method, treatment of pure and mixed cells is separated into two distinct phases. At the beginning of the rezone/remap stage, every mesh node must be marked as pure or mixed. If all cells attached to a node are pure and contain the same material, the node is pure, otherwise it is marked as mixed. For an example of the marking process, see image (a) of Figure 1, where two materials separated by a straight inter-

face are remapped from a randomly perturbed to the equidistant orthogonal mesh.

In the first (pure) stage, only pure nodes are moved in the rezoning process, and the swept remapping is used, see image (b) of Figure 1. As all pure nodes are surrounded by pure cells only, no mixed cell is affected by the mesh motion, and therefore no multi-material cells participate in the swept remap. In the second (mixed) stage, mixed nodes are rezoned, and the intersection-based remapper follows, capable of remapping fluid quantities in the presence of multiple materials, see image (c) of Figure 1. Hence, the existing swept and intersection based remappers are naturally combined without doing anything special between the pure and mixed cells. On the other hand, the buffer cells (layer of pure cells attached to the mixed ones) are treated in both steps, increasing the overhead cost of the 2-step hybrid method. For more details on the 2-step hybrid remapper and its cost analysis, see [3].

3. One-Step Hybrid Remap

The 1-step hybrid remap [7] computes all fluxes at once for quadrilateral meshes. It combines the swept volume fluxes

$$V_{\tilde{c}} = V_c + \sum_{e \in \partial c} \Omega_e \delta V_e = V_c + \sum_{c' \in C(c)} F_{c,c'}^{V,swept} \quad (1)$$

with the intersection based material volume fluxes [11]

$$V_{\tilde{c},k} = V_{c,k} + \sum_{c' \in C(c)} (V_{\tilde{c} \cap c',k} - V_{c \cap \tilde{c}',k}) = V_{c,k} + \sum_{c' \in C(c)} F_{c,c',k}^{V,exact}. \quad (2)$$

Here, c represents a cell in the Lagrangian mesh, \tilde{c} is the corresponding rezoned cell, k is the material index, e is an edge of cell c , and $C'(c)$ is

a set of all neighbors of cell c . δV_e is the swept volume corresponding to edge e , defined by the motion of its vertices to the rezoned positions, and Ω_e is equal to either $+1$ or -1 , depending on the orientation of edge e in cell c . The swept fluxes are equal to zero for corner neighbors, while the intersection-based corner fluxes are present. Let us note that no additional corner coupling error is created, there is no corner flux present in the classical swept approach, while in the exact integration method it is present. The same formulas as in (1) and (2) can be used for the computation of fluxes of other simple integrals, $\int x$ and $\int y$, instead of the flux volume $V = \int 1$. All these integrals can be precomputed at the beginning of the remapping step, and reused for the computation of fluxes of all quantities.

The pure/mixed nodes are marked as in the 2-step hybrid remapper. Next, edge fluxes are marked. An edge flux is pure if both involved vertices are pure, and mixed otherwise, see image (a) of Figure 2. A corner flux is mixed if the involved vertex is mixed, and it is marked as hybrid otherwise. The remapping process sweeps through the cells and through all fluxes in each cell (including the corner ones). For pure/mixed edges, the fluxes are computed by swept/intersection-based remap, as required. For mixed corner fluxes, they are computed by intersections. The remaining hybrid corner fluxes are treated in the following way. If both cell edges attached to this node ($+$ and $-$ in image (b) of Figure 2) are swept, the corner flux is ignored as there is no discrepancy to be fixed. In the opposite case (c), there is a discrepancy between the swept and exact edge fluxes shown as the yellow triangles in image (d) of Figure 2. In this case, we mark the opposite mesh edges by symbols $=$ and \neq . In the case shown in image (d) of Figure 2, we

compute the intersection of the new edge \tilde{e}_{\pm} with the old edge e_{-} (marked in (d) by magenta crosses), construct the triangle surrounded by the intersection and the old and new position of node n , integrate over this triangle, and add this hybrid flux into the mixed flux through e_{-} . The described process helps in most situations with just one exception, when the sideward swept region is non-convex and passes through the node, as shown in Figure 3. This situation is easily detected – only one of four possible mixed intersections $e_{+} \cap \tilde{e}_{-}$, $\tilde{e}_{+} \cap e_{-}$, $e_{-} \cap \tilde{e}_{+}$, and $\tilde{e}_{-} \cap e_{+}$ exists instead of 2 in the standard situation from Figure 2. As before, this triangle must be added to the involved (possibly existent sideward mixed) flux as before, and two cases can occur. If the hybrid node moves outward of the mixed flux (images (a) and (b) of Figure 3), the vertically and horizontally dashed yellow triangles contributed to the mixed flux when treating it from both attached cells, c and c' . These triangles overlap (double dashed yellow triangle in image (b) of Figure 3), so this triangle must be recovered by connecting the old and new nodal position with the extra same-sign intersection $e_{+} \cap \tilde{e}_{+}$, $\tilde{e}_{+} \cap e_{+}$, $e_{-} \cap \tilde{e}_{-}$ or $\tilde{e}_{-} \cap e_{-}$, whichever exists. This contribution must be removed from the mixed edge flux. In the opposite case shown in images (c) and (d) of Figure 3, the hybrid node moves inward, no triangles were added to the mixed flux (they belong to the possible sideward edge flux), and a part of the swept and intersection fluxes overlap. The overlapping triangle is bounded by the nodal coordinates and the existing same-sign intersection, and this contribution must be removed from the mixed flux. This process ensures smooth transition of the intersection-based fluxes to the swept fluxes in the buffer region.

4. Numerical Examples

Here, we present several numerical examples performed using our multi-material remapping research code. All tests start on an equidistant orthogonal mesh in $(0, 1)^2$, 100 random mesh movements followed by the remapping process are performed, and in the last step, the data are remapped back to the initial mesh. The random mesh motion is used as it introduces all possible combinations of edge movements through the material interface and therefore tests the consistency of the remapper. Only material density, volume fractions, and material centroids are remapped in the described flux form. For more details on centroid remap, see [3, 6]. The MOF method [2] was used for material reconstruction in all tests. All tests were performed on a 2.7 GHz AMD Opteron computer.

In the first test, we have remapped a single-material global linear function on meshes with resolutions from 16×16 to 512×512 cells. All tested methods (intersections, 1-step, 2-step hybrid, and even the swept method in this single-material test) prove exact preservation of the linear profile up to the machine accuracy. The time costs (in logarithmic scale) are shown in the upper image of Figure 4. We see that the cost of the hybrid methods is very close to the swept approach, while the one-step hybrid cost almost coincides with the swept cost. The exact intersection-based remapper is significantly more expensive.

In the second test, we have remapped two distinct linear functions in two materials separated by a straight interface, as shown in Figure 1. We omit the swept method in multi-material tests. All methods show exact preservation of a multi-material linear function, even in mixed cells.

Table 1: Material L_1^{mat} error after 100 remapping steps between random meshes of different resolutions, performed by different remapping methods. Data for two different non-linear functions separated by circle interface shown.

Method	16×16	32×32	64×64	128×128	256×256	512×512
intersections	$1.03 \cdot 10^{-2}$	$1.60 \cdot 10^{-3}$	$2.68 \cdot 10^{-4}$	$5.41 \cdot 10^{-5}$	$1.29 \cdot 10^{-5}$	$3.45 \cdot 10^{-6}$
2 step hybrid	$9.32 \cdot 10^{-3}$	$1.48 \cdot 10^{-3}$	$2.49 \cdot 10^{-4}$	$5.32 \cdot 10^{-5}$	$1.32 \cdot 10^{-5}$	$3.56 \cdot 10^{-6}$
1 step hybrid	$9.18 \cdot 10^{-3}$	$1.46 \cdot 10^{-3}$	$2.47 \cdot 10^{-4}$	$5.29 \cdot 10^{-5}$	$1.32 \cdot 10^{-5}$	$3.57 \cdot 10^{-6}$

In the last test, we define a nonlinear density function $10 + (x - \frac{1}{2})^2 + (y - \frac{1}{2})^2$ inside a circle of radius $\frac{1}{4}$ in the center of the domain, and $10 + e^{2xy}$ otherwise. The central circle includes a different material than the rest of the domain, the material interface is therefore curved. The computational cost is shown in the lower image of Figure 4. We can see the benefit of the hybrid approaches when compared with the costly intersections. In Table 1, the numerical errors of material density $\rho_{c,k}$ with respect to the analytic density ($L_1^{\text{mat}} = \sum_{\forall c} \sum_{\forall k \in c} |\rho_{c,k} - \rho(x_{c,k}, y_{c,k})| V_{c,k} / \sum_{\forall c} \sum_{\forall k \in c} \rho(x_{c,k}, y_{c,k}) V_{c,k}$) are shown. Errors originate from two sources – non-linear density and the MOF error due to the curved interface. We observe second order accuracy for all methods, and their errors are comparable.

5. Conclusions

We have described two approaches for combining the swept and intersection-based fluxes in the presence of multiple materials, decreasing the computational cost of the remapper due to costly intersections. To add the 2-step

hybrid method into an existing code, one does not need to do any work on the side of the remapper, changes in the main routine logic are, however, required. The opposite is the case for the 1-step hybrid remapper. Both methods show significant cost improvement when compared with the intersection-based approach, and exhibit numerical errors that are comparable with existing methods for both linear and non-linear densities.

Acknowledgments

This work was performed under the auspices of the National Nuclear Security Administration of the US Department of Energy at Los Alamos National Laboratory under Contract No. DE-AC52-06NA25396. The authors gratefully acknowledge the partial support of the US Department of Energy Office of Science Advanced Scientific Computing Research (ASCR) Program in Applied Mathematics Research and the partial support of the US Department of Energy National Nuclear Security Administration Advanced Simulation and Computing (ASC) Program. The first author was supported by the Czech Ministry of Education grants MSM 6840770022, MSM 6840770010 and LC528, and the Czech Science Foundation project P201/10/P086. Partial support of the BARRANDE MEB021020 program is also gratefully acknowledged.

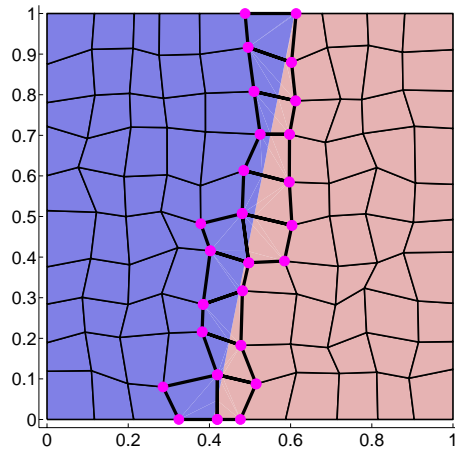
References

- [1] D. J. Benson. Computational methods in Lagrangian and Eulerian hydrocodes. *Computer Methods in Applied Mechanics and Engineering*, 99(2-3):235–394, 1992.

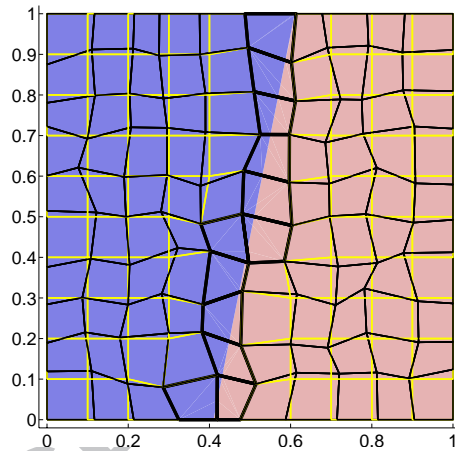
- [2] V. Dyadechko and M. Shashkov. Reconstruction of multi-material interfaces from moment data. *Journal of Computational Physics*, 227(11):5361–5384, 2008.
- [3] S. Galera, M. Kucharik, P.-H. Maire, M. Shashkov, M. Berndt, and J. Breil. Hybrid remapping (conservative interpolation) for multimaterial arbitrary Lagrangian-Eulerian methods. 2010. In preparation.
- [4] C. W. Hirt, A. A. Amsden, and J. L. Cook. An arbitrary Lagrangian-Eulerian computing method for all flow speeds. *Journal of Computational Physics*, 14(3):227–253, 1974.
- [5] P. Kjellgren and J. Hyvarinen. An arbitrary Lagrangian-Eulerian finite element method. *Computational Mechanics*, 21(1):81–90, 1998.
- [6] M. Kucharik, R.V. Garimella, S.P. Schofield, and M.J. Shashkov. A comparative study of interface reconstruction methods for multi-material ALE simulations. *Journal of Computational Physics*, 229(7):2432–2452, 2010.
- [7] M. Kucharik and M. Shashkov. One-step hybrid remapping algorithm for multi-material arbitrary Lagrangian-Eulerian methods. 2010. In preparation.
- [8] M. Kucharik, M. Shashkov, and B. Wendroff. An efficient linearity-and-bound-preserving remapping method. *Journal of Computational Physics*, 188(2):462–471, 2003.
- [9] R. Loubère and M. Shashkov. A subcell remapping method on staggered

polygonal grids for arbitrary-Lagrangian-Eulerian methods. *Journal of Computational Physics*, 209(1):105–138, 2005.

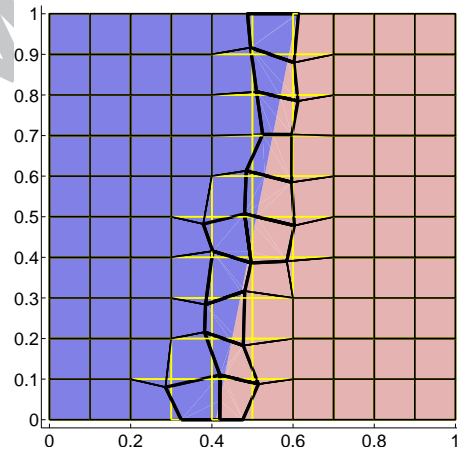
- [10] L. G. Margolin. Introduction to "An arbitrary Lagrangian-Eulerian computing method for all flow speeds". *Journal of Computational Physics*, 135(2):198–202, 1997.
- [11] L. G. Margolin and M. Shashkov. Second-order sign-preserving conservative interpolation (remapping) on general grids. *Journal of Computational Physics*, 184(1):266–298, 2003.
- [12] J. S. Peery and D. E. Carroll. Multi-material ALE methods in unstructured grids. *Computer Methods in Applied Mechanics and Engineering*, 187(3-4):591–619, 2000.



(a) initial



(b) step 1 – pure



(c) step 2 – mixed

Figure 1: Straight interface dividing 2 materials on a randomly perturbed quadrilateral mesh. (a) Initial situation, mixed cells marked by thick edges, mixed nodes by magenta circles. (b) Pure step – pure nodes moved, doing swept remap, new mesh in yellow edges. (c) Mixed step – mixed nodes moved, doing intersection-based remap.

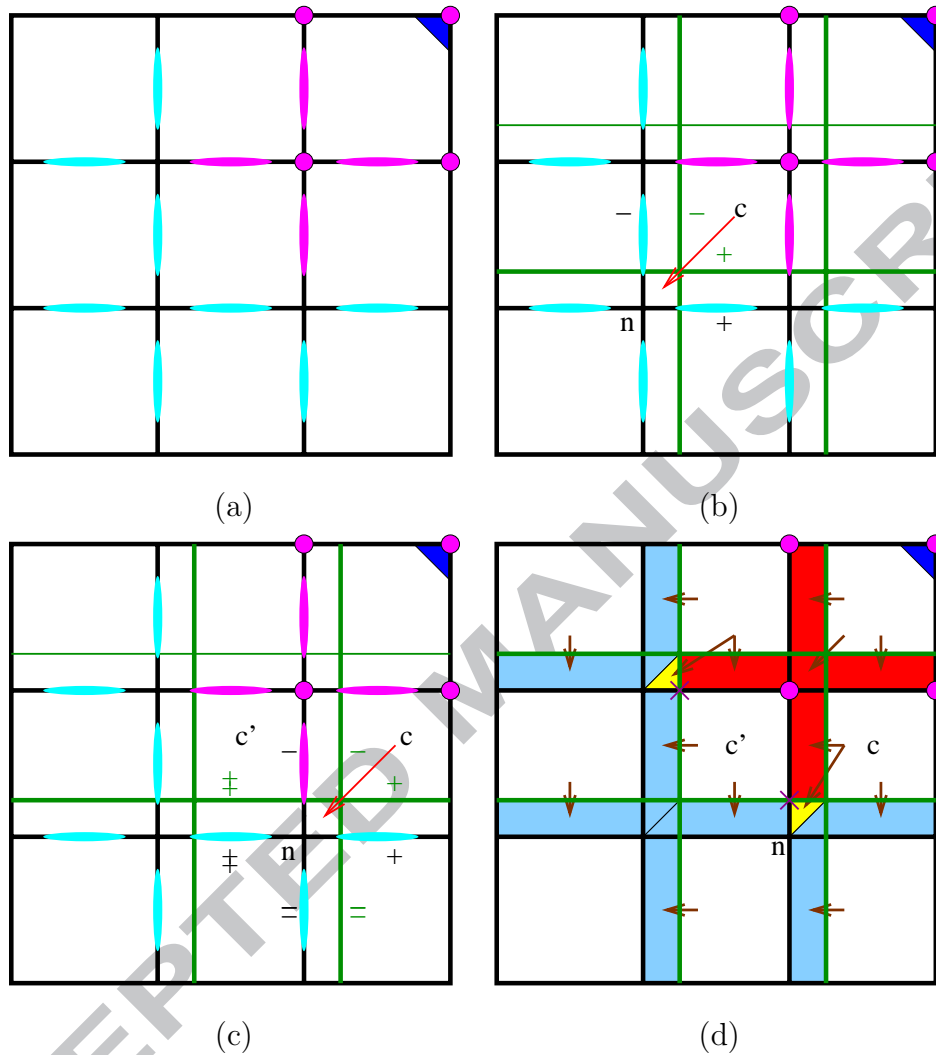


Figure 2: One mixed cell in a multi-material mesh (a) – material segment shown as dark blue triangle, mixed nodes highlighted by magenta circles, and mixed and pure edge fluxes highlighted by magenta and cyan ellipses. Pure node n viewed from cell c (b), as shown by the red arrow, treated by a purely swept approach. Edges of old (black) new (green) meshes annotated by $+$ and $-$ signs with respect to cell c . Hybrid node n viewed from cell c (c), cell c' is neighbor over the hybrid-modified edge. Fluxes (d) computed either by swept movement (light blue) or intersections (red), yellow triangles represent the hybrid correction of the intersection based fluxes. Brown arrows show, from which cell is the reconstruction taken to construct the flux.

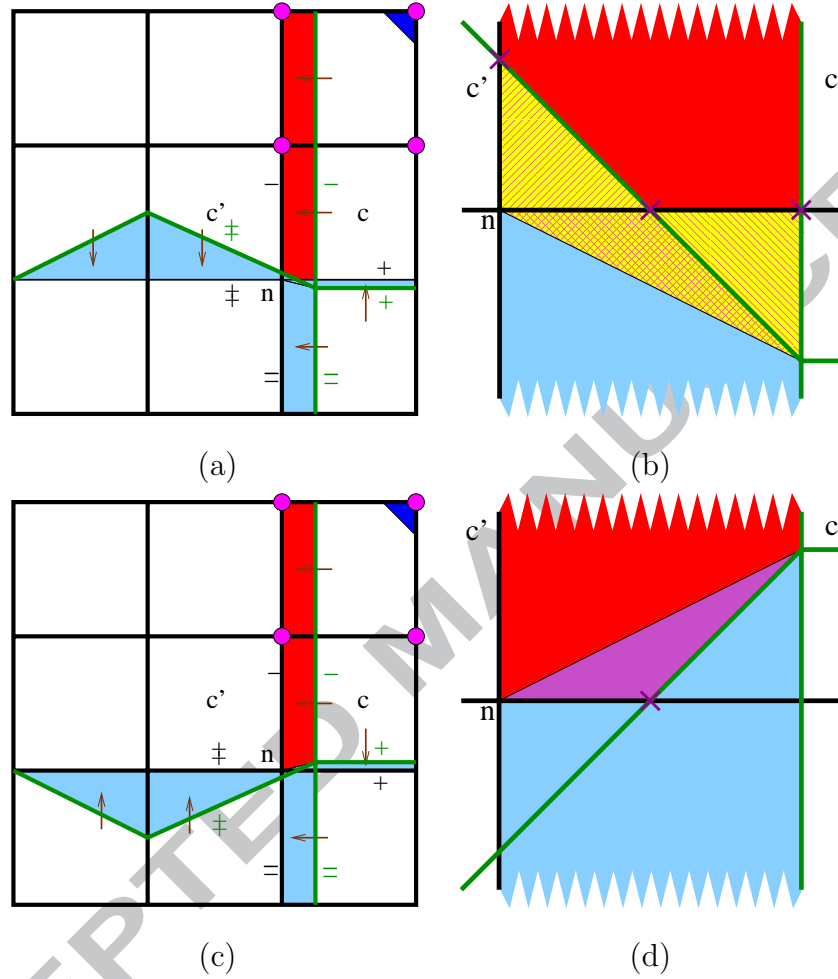


Figure 3: Similar situation as in Figure 2, exceptional situations originated from self-overlapping swept region passing through the hybrid node. Situation (a) – hybrid node moving outward from the intersection treated edge. Sketch (b) (showing only fluxes corresponding to vertical edges) with old and new edge intersections highlighted by magenta crosses, and the hybrid corrections from the yellow triangles (two additional left and right triangles, which overlap and form the central triangle). Situation (c) – hybrid node moving toward the intersection treated edge. Sketch (d) shows the purple triangle where the swept and intersection fluxes overlap.

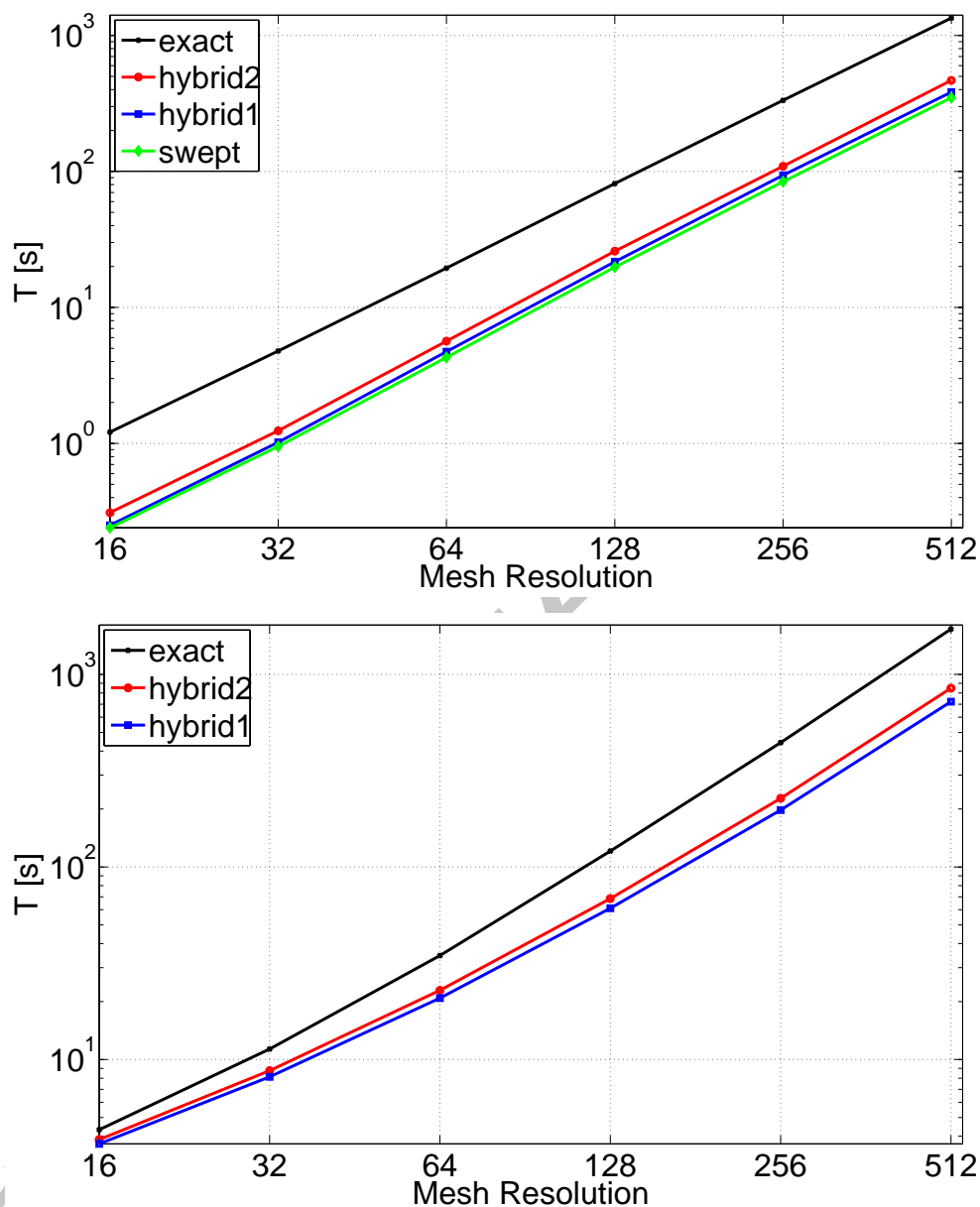


Figure 4: Time of simulation (in seconds) of 100 remapping steps between randomly changing meshes of different resolutions, performed by different remapping methods. Graphs are shown in logarithmic scale for single-material linear function (top) and two different non-linear functions separated by circle interface (bottom).